# Development Threat Index, version 1

## Metadata for All Data Layers

This metadata document contains the methodological descriptions for the cumulative Development Threat Index and each of the nine input layers: Agricultural Expansion, Biofuels, Coal, Conventional Oil and Gas, Mining Solar, Unconventional Oil and Gas, Urban Expansion, and Wind.

The document is a complement to the peer reviewed article: Oakleaf, J. R., C. M. Kennedy, S. Baruch-Mordo, P. C. West, J. S. Gerber, L. Jarvis, and J. Kiesecker. 2015. A World at Risk: Aggregating Development Trends to Forecast Global Habitat Conversion. *PLoS ONE* 10(10): e0138334. https://doi.org/10.1371/journal.pone.0138334.

SEDAC Data Set Citation: Oakleaf, J. R., C. M. Kennedy, S. Baruch-Mordo, P. C. West, J. S. Gerber, L. Jarvis, and J. Kiesecker. 2019. *Development Threat Index, v1*. Palisades, NY: NASA Socioeconomic Data and Applications Center (SEDAC). https://doi.org/10.7927/61jv-th84.

# *Global Future Development Threat:*

## *Cumulative Development Threat from Agricultural Expansion, Urban Expansion, Conventional & Unconventional Oil and Gas, Coal, Mining, Biofuels, Solar, and Wind*

**Description:** We created a terrestrial global, future development threat map based on combining nine types of development: agricultural and urban expansion, conventional and unconventional oil and gas development, coal mining, mineral and earthen material extraction, and renewable energy development (i.e. biofuels, solar and wind production). For mapping all nine development threats, we relied on publically available global datasets and assessed development risk based on potential, unexploited resources (see individual methods documents). For each threat, we mapped potential development, which was ranked from 0-100 with 100 indicating the highest potential for future development of the resource. All maps were produced at a 50 $km^2$ grid cell resolution, excluding all cells overlapping Antarctica and those with >50% considered marine. This resulted in a total of 53,863 cells included in our analysis.

**Global Future Threat Assessment - Methods Overview:** To determine cumulative, future development threat map, we first ranked all nine layers (see each individual layer raking methods) and then summed these values to produce a cumulative ranking. We then scaled this cumulative ranking using a spatial percentile-rank method (Oakleaf, Kennedy, Boucher, & Kiesecker, 2013), also known as equal-area ranks, using the following formula:

$$\frac{c_i + 0.5 f_i}{N} * 100$$

where $c_i$ is the count of all grid cells with values less than the target cell value, $f_i$ is the number of cells with the target cell value, and $N$ is the total number of cells in the study extent. To produce the final cumulative ranking, we rescaled the area rank scores using a min/max normalization to ensure consistency such that cells without any threats were 0 and the highest threat cells were 100. After summing the development ranks across all development sectors, we identified the top cumulative, ranked cells covering 25% of earth's land area, and categorized these regions as having high future development risk. We selected the top quarter as the cut-off to delineate areas of the globe at high future development risk. We examined the sensitivity of this cut-off by comparing 5%, 10%, and 25% cut-offs and found high correlations between percent development risk by ecoregion for these different cut-offs (Pearson's $r \geq 0.98$, analyses not shown).

**Global Map of Future, Cumulative Development Threat:**

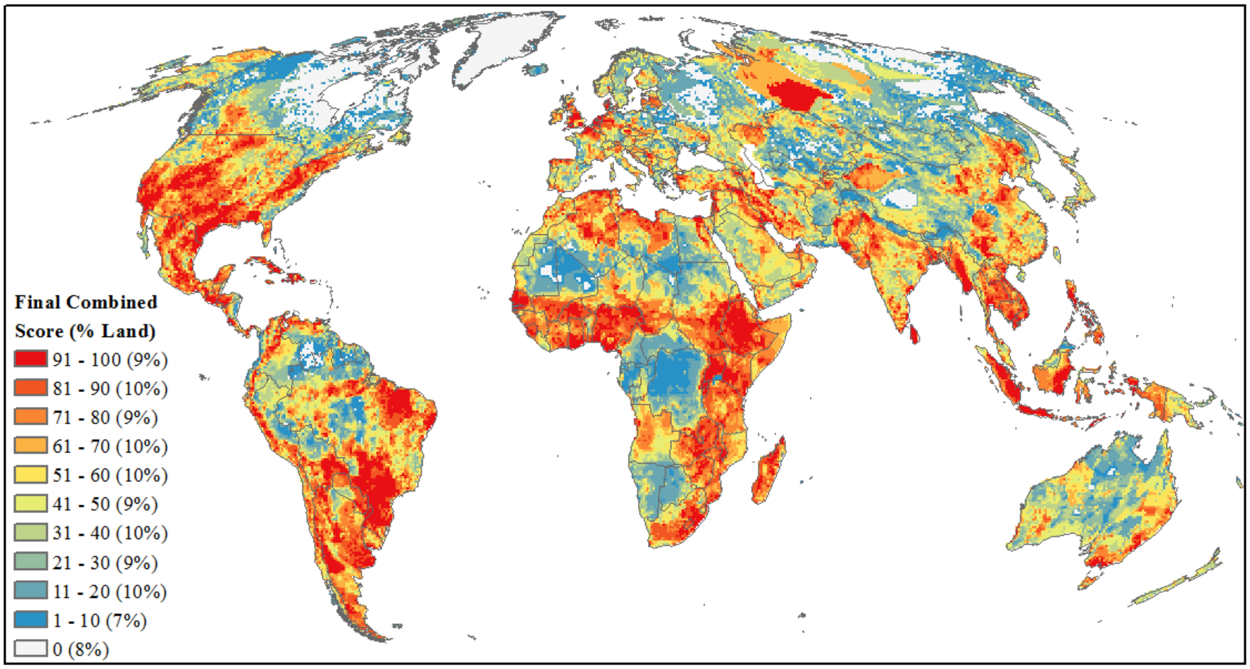


**Detailed Data Processing Steps:**

1. Summed the ranks of all nine threat layers (i.e. agricultural expansion, urban expansion, conventional oil and gas, unconventional oil and gas, coal, mining, biofuels, solar, and wind).
2. Equal-area ranked the total, summed values.
3. Min/max normalization from 0-100 the equal-area ranked values.

**Data Access:** http://s3.amazonaws.com/DevByDesign-Web/MappingAppsVer2/DevRisk/index.html

**Citation:** Oakleaf JR, Kennedy CM, Baruch-Mordo S, West PC, Gerber JS, Jarvis L, Kiesecker J (2015) A world at risk: Aggregating development trends to forecast global habitat conversion. PLoS ONE.

**Contact for Development Risk Data:**

Jim Oakleaf, Conservation Geographer
Development by Design, The Nature Conservancy
joakleaf@tnc.org

**References:**

Oakleaf, J., Kennedy, C., Boucher, T., & Kiesecker, J. (2013). Tailoring Global Data to Guide Corporate Investments in Biodiversity, Environmental Assessments and Sustainability. *Sustainability*, *5*(10), 4444–4460. doi:10.3390/su5104444

## *Future Development Threat from Agricultural Expansion*

**Resource Description:** Agricultural land occupies 38% of the world's terrestrial surface, with pasture making up 26% and crops another 12% of the Earth's ice-free land (Monfreda, Ramankutty, & Foley, 2008). As populations and income rise so does the demand for food, which could be met by the intensification of existing agricultural lands and/or the conversion of natural lands (Licker et al., 2010). Currently, the largest driver of the conversion of natural habitats is the expansion of agriculture (UNEP, 2009). Current estimates for 2050 range from 350 million ha (i.e. 7% increase) to 1,500 million ha (i.e. 31% increase) expansion of agriculture, predominately in developing countries within South America, Africa and Asia (UNEP, 2014).

**Relative Future Threat Assessment - Methods Overview:** Using a gridded time series of globally mapped cropland and pasture from 1961-2011 (Ramankutty & Foley, 2014), we calculated total agricultural area as the sum of the fractional area of cropland and pasture within grid cells at 5 arc-minute resolution (~9km X 9km at the equator). We then summed the cropland and pasture fractional area for each pixel and time step (i.e. year) to calculate total agricultural area. For each pixel, we calculated the recent rate of agricultural expansion as the slope of the linear least-square fit regression from 2000 to 2011. Given our analysis focuses on the potential threat of future development, we considered only areas with positive rates of agricultural expansion, relating to natural areas with potential for conversion; we did not consider negative rates, which related to the recovery of abandoned lands.

To simulate expansion of cropland or pasture, we re-gridded the data to 30-minute resolution and allowed for spillover into neighboring pixels. With this approach we project agricultural expansion only into areas that are within approximately within 60 km of existing agricultural lands. The expansion rate was calculated as the average expansion rate for all positive-slope 5-min grid cells within each 30-minute grid cell. The resulting data were the annual rates (fractional area per year) for each pixel. The 30-minute average expansion rates were re-gridded to 5-minute resolution and projected to a Mollweide equal-area projection using bilinear interpolation. To project the fractional area of agricultural expansion for 2030, we assumed a linear rate increase based on calculated annual rates. In cases where the fractional area of agricultural expansion for 2030 plus current agricultural land (Ramankutty & Foley, 1999, 2014) and urban areas (Schneider, Friedl, & Potere, 2009) summed to greater than one (i.e. greater than the entire grid cell), the final fractional area for 2030 agricultural expansion was calculated by subtracting both fractional areas of current agriculture and urban areas from one. To ensure consistency with other development threat layers, we calculated the mean fractional area of agricultural expansion for 2030 for a 50 km grid cell and area-ranked these values from 1-100.

**Global Map of Future Agricultural Expansion Development Threat:**

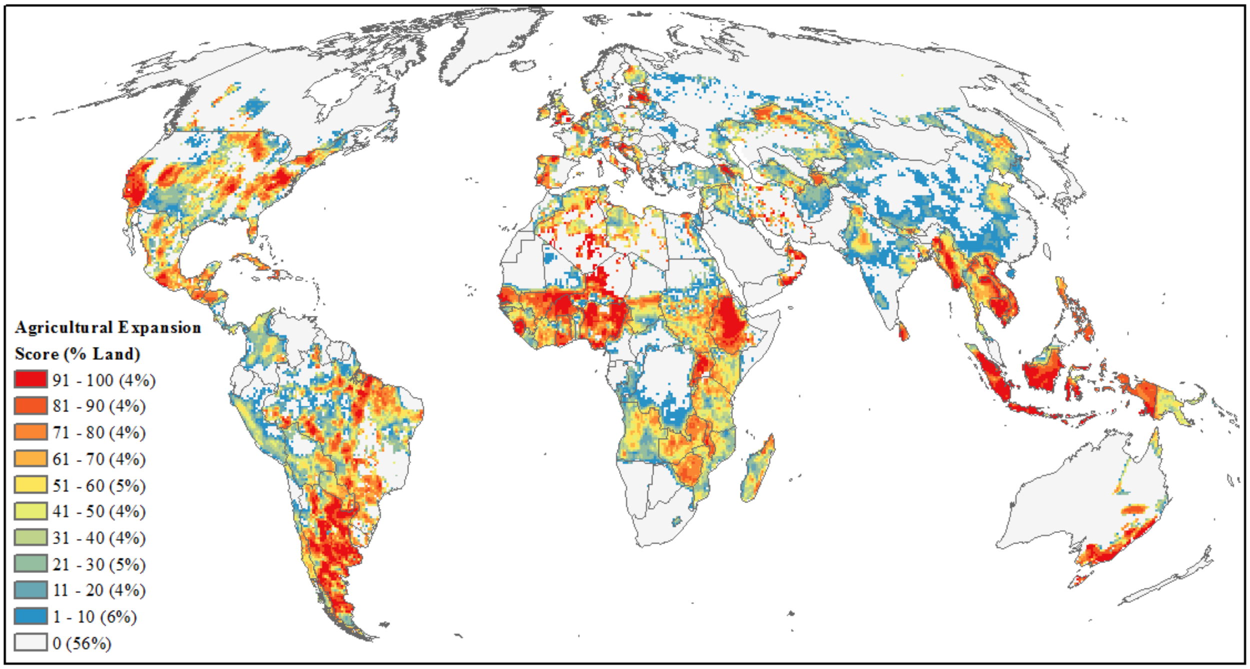


**Detailed Data Processing Steps:**

1. Calculated total agricultural area as the sum of the fractional area of cropland and pasture within grid cells at 5 arc-minute resolution (~9km X 9km at the equator) for a gridded time series of croplands and pastures from 1961-2011 (Ramankutty & Foley, 1999, 2014).
2. Calculated the recent rate of expansion for each pixel as the slope of the linear least-square fit regression from 2000 to 2011.
3. Set to null grid cells with negative rates.
4. Resampled data to 30-minute resolution and calculated the average expansion rate for all positive-slope 5-min grid cells within each 30-minute grid cell.
5. Resampled the 30-minute average expansion rates back to 5-minute resolution.
6. Averaged expansion rates at the 5-min resolution were projected to Mollwiede using bilinear interpolation with a 10 km resolution.
7. For each grid cell, used a linear rate of increase and calculated the fractional area of agricultural expansion for 2030 (i.e. 19 * rate).
8. Calculated the *fractional area of current urban* using Schneider, et al (2009).
9. Projected the *fractional area of agricultural land for 2011* (Ramankutty & Foley, 1999, 2014) to Mollwiede using bilinear interpolation with a 10 km resolution.
10. Applied the following conditional statements to calculate the final fractional area of agricultural expansion for 2030:
    a. If: *Fractional area of agricultural expansion for 2030 + fractional area of current urban + fractional area of agricultural land for 2011 > 1*
        i. Then: Final 2030 fractional area of agricultural expansion = 1 - *fractional area of current urban - fractional area of agricultural land for 2011*

ii. Else: Final fractional area of agricultural expansion for 2030 = *fractional area of agricultural expansion for 2030 .*

11. Calculated mean fractional area of agricultural expansion for 2030 at 50km resolution.
12. Created a final area-rank from 1-100 the using the mean fractional area of agricultural expansion for 2030.

**Data Access:** [http://s3.amazonaws.com/DevByDesign-Web/MappingAppsVer2/DevRisk/index.html](http://s3.amazonaws.com/DevByDesign-Web/MappingAppsVer2/DevRisk/index.html)

**Citation:** Oakleaf JR, Kennedy CM, Baruch-Mordo S, West PC, Gerber JS, Jarvis L, Kiesecker J (2015) A world at risk: Aggregating development trends to forecast global habitat conversion. PLoS ONE.

**Contact for Development Risk Data:**

Jim Oakleaf, Conservation Geographer
Development by Design, The Nature Conservancy
joakleaf@tnc.org

**References:**

Licker, R., Johnston, M., Foley, J. A., Barford, C., Kucharik, C. J., Monfreda, C., & Ramankutty, N. (2010). Mind the gap: how do climate and agricultural management explain the "yield gap" of croplands around the world? *Global Ecology and Biogeography*, *19*(6), 769–782. doi:10.1111/j.1466-8238.2010.00563.x

Monfreda, C., Ramankutty, N., & Foley, J. (2008). Farming the planet: 2. Geographic distribution of crop areas, yields, physiological types, and net primary production in the year 2000. *Global Biogeochemical Cycles*, *22*(Journal Article), GB1022–GB1022.

Ramankutty, N., & Foley, J. A. (1999). Estimating historical changes in global land cover: Croplands from 1700 to 1992. *Global Biogeochemical Cycles*, *13*(4), 997–1027. doi:10.1029/1999GB900046

Ramankutty, N., & Foley, J. A. (2014). Historical Cropland and Pasture from 1700 - 2011 - Update. Retrieved February 15, 2014, from http://www.earthstat.org/48-2/download/data/#Crop_and_pasture_area_from_1700_to_2007

Schneider, A., Friedl, M., & Potere, D. (2009). A new map of global urban extent from MODIS data. *Environmental Research Letters*, *4*. Retrieved from http://sage.wisc.edu/people/schneider/research/data.html

UNEP. (2009). *The environmental food crisis - The environment's role in averting future food crises.* Retrieved from http://www.grida.no/files/publications/FoodCrisis_lores.pdf

UNEP. (2014). *Assessing Global Land Use: Balancing Consumption with Sustainable Supply. A Report of the Working Group on Land and Soils of the International Resource Panel.* (p. 132). Retrieved from http://www.unep.org/resourcepanel/Portals/24102/PDFs//Full_Report-Assessing_Global_Land_UseEnglish_(PDF).pdf

# *Future Development Threat for Biofuels*

**Resource Description:** Biofuels are liquid fuels, mainly ethanol or biodiesel, made from organic matter (International Energy Agency, 2011). Ethanol is largely created from sugar- and starch-based feed stocks such as sugarcane and corn. Biodiesel is derived from oil crops such as rapeseed, soybean, oil palm, and sunflower. Biofuels currently make up 3% of global road transport fuels but could provide up to 27% in 2050 (International Energy Agency, 2011). In order to meet this increase proportion, expansion of cropland would have to increase anywhere from 48 million ha to 80 million hectares (UNEP, 2014). Currently US and Brazil dominate in production of biofuels with a total global share of 45% and 23% respectively (BP, 2013).

**Relative Future Threat Assessment - Methods Overview:** A cumulative threat assessment for biofuels produced from six crops (maize, soybean, sugarcane, rapeseed, sunflower, and palm oil) was created based on two factors: projected cropland expansion and potential biofuel production. We focused on the top first generation biofuel crops (over second generation biofuels) given they have mature commercial markets and well-understood technologies, make up the vast majority of commercial biofuel production (IEA 2008) and have the potential to accelerate indirect land use change (Fargione et al. 2010).

*Cropland Expansion:* Using a gridded time series of croplands from 1961-2011(Ramankutty & Foley, 2014), we calculated total cropland area as the fractional area of cropland at 5 arc-minute resolution (~9km X 9km at the equator). We then calculated the recent rate of expansion for each pixel as the slope of the linear least-square fit regression from 2000 to 2011 based on positive slopes. Negative rates were discarded to focus on the conversion of existing natural habitat (and not recovery of abandoned land).

To allow for cropland expansion into neighboring pixels, we re-gridded the data to a 30-minute resolution. The expansion rate was calculated as the average expansion rate for all positive-slope 5-min grid cells within each 30-minute grid cell. The resulting data were the annual rates (fractional area per year) for each pixel. The 30-minute average expansion rates were re-gridded to 5-minute resolution to be consistent with the other biofuel input data. To project the fractional area of cropland expansion for 2030, we assumed a linear rate increase based on calculated annual rates. In cases where the fractional area of cropland expansion for 2030 plus current cropland (based on (Ramankutty & Foley, 1999, 2014) and current urban areas (Schneider, Friedl, & Potere, 2009) summed to greater than one (i.e. greater than the entire grid cell), the final fractional area cropland expansion for 2030 was calculated by subtracting both fractional areas of current cropland and urban areas from one.

*Potential Biofuel Production:* Potential biofuel production was calculated using a yield gap approach for determining attainable yields (tons per hectare) based on climate conditions and agricultural census data (Licker et al., 2010; Mueller et al., 2012). Potential yields were defined as the 95$^{th}$ percentile yield within 100 crop-specific climate bins. For consistency, all yields were converted to gallons of gasoline equivalents (GGEs) (Table 1). We then estimated potential expansion of each biofuel crop based on the climatic growing conditions. The potential extent for each biofuel crop was calculated by mapping its "climate envelope" (limited by the 100 climate bins delineated in the previous step) onto all land. The driest climate bin at each temperature range was removed from the analysis as they represent extreme growing conditions that would require very intensive irrigation (such as the Sahara Desert and the interior of Australia). A global, maximum potential GGE map was produced by combining all six biofuel crops and maintaining the highest GGE value where crops overlapped.

**Table 1. Conversion from crop yields (tons) to fuel (gasoline gallon equivalents):**

| Crop Name | Ethanol (liter/ton)* | biodiesel (liter/ton)* | Conversion (liter to gallon) | Biofuels to GGE ** | Conversion tons to GGE |
|---|---|---|---|---|---|
| Maize | 410 | | 0.264172 | 1.5 | 162.47 |
| Sugarcane | 81 | | 0.264172 | 1.5 | 32.10 |
| Oil Palm | | 223 | 0.264172 | 0.96 | 56.55 |
| Rapeseed | | 392 | 0.264172 | 0.96 | 99.41 |
| Soybean | | 183 | 0.264172 | 0.96 | 46.41 |
| Sunflower | | 418 | 0.264172 | 0.96 | 106.01 |

*(Johnston et al., 2011)

**("Fuel Energy Comparisions: Gasoline Gallon Equivalents (GGE)," n.d.)

*Final Biofuel Threat Ranking*: To create a final biofuels threat map, we produced a potential GGE expansion map by multiplying the factional area of cropland expansion in 2030 by the maximum potential GGE. This procedure modifies GGE values in areas based on their likelihood of future cropland expansion, which results in attributing maximum potential GGE values to areas where the likelihood of agricultural expansion is 1 and attributes GGE value of 0 in areas without likely future expansion. We then summed these potential GGE expansion values within a 50 km grid cell and area-ranked these values from 1-100.

**Global Map of Future Biofuels Development Threat:**

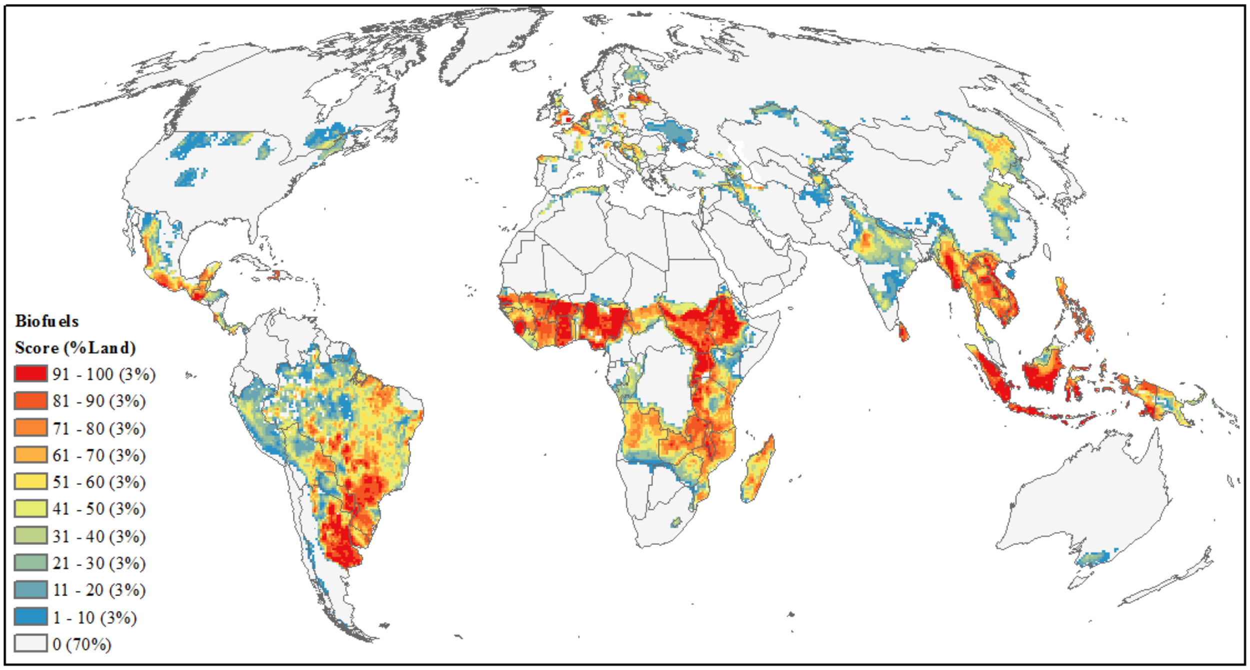


**Detailed Data Processing Steps:**

Task 1: Cropland Expansion

1. Used the fractional area of cropland within grid cells at 5 arc-minute resolution (~9km X 9km at the equator) for a gridded time series of croplands from 1961-2011 (Ramankutty & Foley, 1999, 2014)
2. Calculated the recent rate of expansion for each pixel as the slope of the linear least-square fit regression from 2000 to 2011.
3. Set to null grid cells with negative rates.
4. Resampled data to 30 minute resolution and calculated the average expansion rate for all positive-slope 5-min grid cells within each 30-minute grid cell.
5. Resampled the 30-minute average expansion rates back to 5-minute resolution.
6. Average expansion rates at the 5-min resolution were projected to Mollwiede using bilinear interpolation with a 10 km resolution.
7. For each grid cell, used a linear rate of increase and calculated the *cropland fractional area expansion for 2030* (i.e. 19 * rate).
8. Calculated *current fractional area of urban* using Schneider, et al (2009).
9. Projected the *fractional area of cropland for 2011* (Ramankutty & Foley, 1999, 2014) to Mollweide using bilinear interpolation with a 10 km resolution.
10. Applied the following conditional statements to calculate the final fractional area of cropland expansion for 2030:

a. If: *Fractional area of cropland expansion for 2030 + fractional area of current urban + fractional area of cropland for 2011 > 1*
   i. Then: Final 2030 fractional area of cropland expansion = 1 - *fractional area of current urban - fractional area of cropland for 2011*
   ii. Else: Final 2030 fractional area of cropland expansion = *cropland fractional area expansion for 2030*

Task 2: Potential Biofuel Production

1. Calculated current maximum potential yields in tons per ha for six biofuel crops (maize, soybean, sugarcane, rapeseed, sunflower, and oil palm) based on climate conditions and agricultural census data (Licker et al., 2010; Mueller et al., 2012).
2. Multiplied yield in tons by crop specific conversion rates to GGE (Table 1, column 6).
3. Mapped the potential extent for all six biofuel crops using its "climate envelope", limited by 100 crop-specific climate bins.
4. Removed driest climate bin at each temperature range.
5. Produced a global, maximum potential GGE map by combining all six biofuels crops and maintaining the highest GGE value where different crops overlapped.

Task 3: Final Biofuel Threat Ranking

1. Created potential GGE expansion = fractional area of cropland expansion for 2030 * maximum potential GGE.
2. Summed potential GGE expansion within 50km cells.
3. Area ranked from 1-100 using the summed values.

**Data Access:** http://s3.amazonaws.com/DevByDesign-Web/MappingAppsVer2/DevRisk/index.html

**Citation:** Oakleaf JR, Kennedy CM, Baruch-Mordo S, West PC, Gerber JS, Jarvis L, Kiesecker J (2015) A world at risk: Aggregating development trends to forecast global habitat conversion. PLoS ONE.

**Contact for Development Risk Data:**
Jim Oakleaf, Conservation Geographer
Development by Design, The Nature Conservancy
joakleaf@tnc.org

**References:**

BP. (2013). Statistical Review of World Energy 2013. Retrieved April 10, 2014, from http://www.bp.com/en/global/corporate/about-bp/energy-economics/statistical-review-of-world-energy-2013.html

Fuel Energy Comparisions: Gasoline Gallon Equivalents (GGE). (n.d.). Retrieved April 11, 2014, from http://alternativefuels.about.com/od/resources/a/gge.htm

International Energy Agency. (2011). *Technology Roadmap: Biofuels for Transport* (p. 50). Retrieved from http://www.iea.org/publications/freepublications/publication/Biofuels_Roadmap_WEB.pdf

Johnston, M., Licker, R., Foley, J. A., Holloway, T., Mueller, N., Barford, C., & Kucharik, C. J. (2011). Closing the gap: global potential for increasing biofuels production through intensification. *Environmental Research Letters*, *6*(3), 34028. Retrieved from http://stacks.iop.org/1748-9326/6/i=3/a=034028

Licker, R., Johnston, M., Foley, J. A., Barford, C., Kucharik, C. J., Monfreda, C., & Ramankutty, N. (2010). Mind the gap: how do climate and agricultural management explain the "yield gap" of croplands around the world? *Global Ecology and Biogeography*, *19*(6), 769–782. doi:10.1111/j.1466-8238.2010.00563.x

Mueller, N. D., Gerber, J. S., Johnston, M., Ray, D. K., Ramankutty, N., & Foley, J. A. (2012). Closing yield gaps through nutrient and water management. *Nature*, *490*(7419), 254–257. doi:10.1038/nature11420

Ramankutty, N., & Foley, J. A. (1999). Estimating historical changes in global land cover: Croplands from 1700 to 1992. *Global Biogeochemical Cycles*, *13*(4), 997–1027. doi:10.1029/1999GB900046

Ramankutty, N., & Foley, J. A. (2014). Historical Cropland and Pasture from 1700 - 2011 - Update. Retrieved February 15, 2014, from http://www.earthstat.org/48-2/download/data/#Crop_and_pasture_area_from_1700_to_2007

Schneider, A., Friedl, M., & Potere, D. (2009). A new map of global urban extent from MODIS data. *Environmental Research Letters*, *4*. Retrieved from http://sage.wisc.edu/people/schneider/research/data.html

UNEP. (2014). *Assessing Global Land Use: Balancing Consumption with Sustainable Supply. A Report of the Working Group on Land and Soils of the International Resource Panel.* (p. 132). Retrieved from http://www.unep.org/resourcepanel/Portals/24102/PDFs//Full_Report-Assessing_Global_Land_UseEnglish_(PDF).pdf

## *Future Development Threat for Conventional Oil and Gas*

**Resource Description:** Conventional oil and natural gas (OG) are resources extracted via drilling techniques that tap into reservoirs below the Earth's surface and are collected using the natural pressure found in the reservoir or through pumping (Behrens, Ratner, & Glover, 2011). The quantities of OG can be categorized as proven reserves or undiscovered resources with volumetric units in barrels for oil and natural gas liquids (NGL) and cubic feet for dry natural gas. Proven reserves are known OG volumes that are currently economically recoverable using current OG drilling practices. Undiscovered resources are estimated OG volumes based on geological characteristics similar to currently producing geologic formations (Behrens et al., 2011), and their volumes are estimated by a computer simulation that predicts a range of possible volumes based on extraction probabilities (Charpentier & Cook, 2010). An overall mean estimated volume from these predictions is reported for each of the assessment units (AUs), which are totaled for an entire geological province (area with similar geological characteristics). Globally, there are 939 geological provinces with 401 of these provinces having conventional OG resources (Klett, Ahlbrandt, Schmoker, & Dolton, 1997). Over 100 countries are producing OG worldwide, many of which assess their reserves annually to determine the current and potential OG resources (US Energy Information Administration (EIA), 2014). Globally the US Geological Survey (USGS) has made extensive efforts to survey all provinces that comprise 95% of the current World's OG known reserves and other provinces with potential for large amounts of undiscovered OG resources (US Geological Survey, 2000, 2012b). These global assessments along with national-level assessments for the U.S. (US Geological Survey, 2012a) and Australia (Geoscience Australia, 2011) provide undiscovered volumes for OG resources for a total of 305 geologic provinces.

**Relative Future Threat Assessment - Methods Overview:** To produce a relative future development threat estimate for conventional OG, we combined the two global OG assessments (US Geological Survey, 2000, 2012b) with the Australia and U.S. national OG assessments (Geoscience Australia, 2011; US Geological Survey, 2012a) and ranked provinces based on the most recent undiscovered OG resource estimates. We only used estimates of undiscovered resources in our ranking because these resources have yet to be exploited and identify where future OG development may occur. We calculated the total undiscovered OG resources by calculating the million barrels of oil equivalent (MBOE) for each resource (oil, gas, and natural gas liquids) and summing them together for each geological province. We restricted our analysis to terrestrial-based lands and selected those provinces identified as having onshore development (Horn, 2005; Lujala, Rod, & Thieme, 2007) or having at least 50% of the province overlapping land. This selection resulted in 242 provinces with undiscovered OG resources. Using the MBOE values of these provinces, we then migrated these data to a raster dataset having a 50 $km^2$ cell size. For our analysis we only considered 50 $km^2$ cells overlapping at least 50% of the ranked province and excluded any portion of the province overlapping a marine environment. Finally we area-ranked from 1-100 cells having a MBOE value.

**Global Map of Future Conventional Oil and Gas Development Threat:**

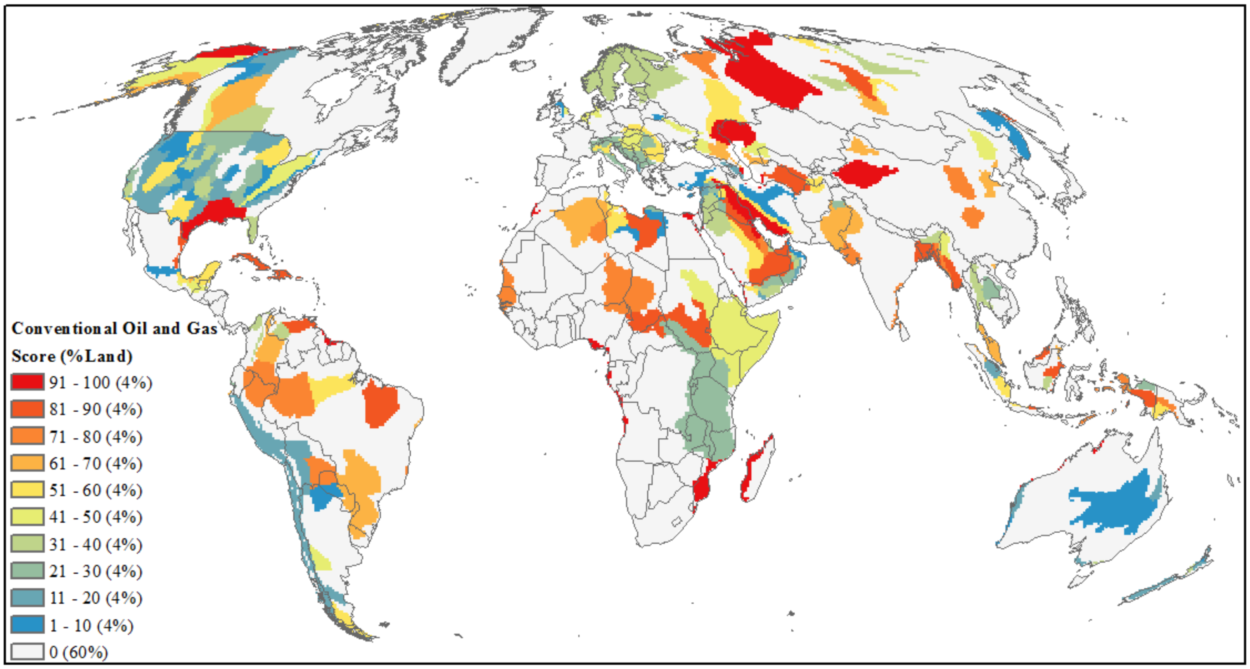


**Detailed Data Processing Steps:**

1. Obtained oil and gas resource information from the following sources, which produced 305 provinces with undiscovered volumes of oil, gas and natural gas liquids:

    a. 2000 USGS Global Assessment (USGS 2000) – assessed 132 provinces for undiscovered volumes (used 24 provinces which were not updated in 2012)

    b. 2012 USGS Global Assessment (USGS 2013b) – assessed or re-assessed 215 provinces for undiscovered volumes (re-assessed 108 out of the 132 provinces assessed in 2000 and added 107 new provinces)

    c. 2011 Australia Assessment (Geoscience Australia 2011) – provided undiscovered volumes for 8 provinces not assessed by USGS

    d. 2013 USGS US Assessment (USGS 2013b) – provided updated information for 58 provinces found in the US with conventional oil and gas reserves. Only identifies undiscovered amount of resources

2. Merged all provinces into one layer (totaling 305 provinces). Maintained fields for undiscovered oil, gas, NLG volumes (all mean predicted volumes) and calculated the overall MBOE value by first computing the MBOE of natural gas (i.e. billion cubic feet of natural gas/6) and summing this value with the million barrels of oil and NGL.

3. Removed provinces with volumes of 0 undiscovered resources (8 provinces) given their negligible development potential (resulting in 297 provinces)

4. Removed any province with only off-shore oil or gas development (as identified by either Horn 2005 or Lujala et al 2007) and those provinces without having at least 50% of the province overlapping land. This led to the removal of 55 provinces (resulting in 242 provinces)

5. Migrated the MBOE values associated with the 242 polygon-based provinces to a raster format at a 50 $km^2$ cell resolution. Only cells with at least 50% of the province overlapping the cell were kept. Additionally our analysis removed any cell with 50% or more of the cell overlapping a marine environment.

6. Area-ranked from 1-100 cells having an MBOE value.

**Data Access:** http://s3.amazonaws.com/DevByDesign-Web/MappingAppsVer2/DevRisk/index.html

**Citation:** Oakleaf JR, Kennedy CM, Baruch-Mordo S, West PC, Gerber JS, Jarvis L, Kiesecker J (2015) A world at risk: Aggregating development trends to forecast global habitat conversion. PLoS ONE.

**Contact for Future Development Threat Data:**
Jim Oakleaf, Conservation Geographer
Development by Design, The Nature Conservancy
joakleaf@tnc.org

**References:**

Behrens, C. E., Ratner, M., & Glover, C. (2011). *U . S . Fossil Fuel Resources : Terminology , Reporting , and Summary* (pp. 1–25). Retrieved from https://www.fas.org/sgp/crs/misc/R40872.pdf

Charpentier, R., & Cook, T. (2010). Improved USGS methodology for assessing continuous petroleum resources. *US Geological Survey Data Series*. Retrieved from http://pubs.usgs.gov/ds/547/downloads/DS547v2.pdf

Geoscience Australia. (2011). Petroleum Reserves by Basin as at 1 Jan 2011. Retrieved January 15, 2014, from http://www.ga.gov.au/products-services/publications/oil-gas-resources-australia/2010/reserves/table-1.html

Horn, M. (2005). Giant oil and gas fields. *American Association of Petroleum Geologists*, *Open Acces*. Retrieved from http://www.datapages.com/AssociatedWebsites/GISOpenFiles/HornGiantFields.aspx

Klett, T. R., Ahlbrandt, T. S., Schmoker, J. W., & Dolton, G. L. (1997). *Ranking of the World's Oil and Gas Provinces by Known Petroleum Volumes*. Retrieved from http://pubs.usgs.gov/dds/dds-069/dds-069-ff/downloads/

Lujala, P., Rod, J. K., & Thieme, N. (2007). Fighting over Oil: Introducing A New Dataset. *Conflict Management and Peace Science*, *24*(3), 239–256. Retrieved from http://www.prio.no/Data/Geographical-and-Resource-Datasets/Petroleum-Dataset/Petroleum-Dataset-v-12/

US Energy Information Administration (EIA). (2014). International Energy Statistics: Reserves of Oil and Natural Gas for 2012. Retrieved March 15, 2014, from http://www.eia.gov

US Geological Survey. (2000). World Petroleum Assessment 2000. Retrieved September 15, 2013, from http://pubs.usgs.gov/dds/dds-060/

US Geological Survey. (2012a). National Oil and Gas Assessment 2012 Assessment Updates. Retrieved September 01, 2013, from http://energy.usgs.gov/OilGas/AssessmentsData/NationalOilGasAssessment/AssessmentUpdates.aspx

US Geological Survey. (2012b). USGS 2012 World Assessment of Undiscovered Oil and Gas Resources. Retrieved December 15, 2013, from http://pubs.usgs.gov/dds/dds-069/dds-069-ff/

# *Future Development Threat for Mining*

**Resource Description:** Mining is the surface or sub-surface excavation of mineral deposits and/or other geologic materials deposited in the Earth. Surface mining requires the removal of vegetation, soils and layers of bedrock to reach deposits whereas in underground mining a tunnel is created to reach the deposit. Globally more than 70 chemical elements and dozens of minerals are mined and produced from over 100 different deposits (Schulz & Briskey, 2003). World demand of minerals, expected to rise by 60% by 2050, is based on three factors: new and increased uses of minerals, growing populations, and increased wealth (Kesler, 2007). Currently China is the largest producer for 44 commodities and among the top three for 12 additional commodities out of a total of 73 globally tracked (British Geological Survey, 2012).

**Relative Future Threat Assessment - Methods Overview:** We relied on three main sources to determine development threat related to mining: 1) Global Mineral Resources Data System (MRDS)(US Geological Survey, 2005), 2) Global Minerals Deposits update of 2011 (Causey, Galloway, & Zientek, 2009; Cox, Lindsey, Singer, Moring, & Diggles, 2007; Singer, Berver, & Moring, 2008) and 3) World Geoscience Database (Geologic Survey of Canada, 2005). These three datasets were combined into one identifying unexploited deposits. To discern patterns of future potential development, we removed current or past mining locations and any duplicate locations of the same mineral. This resulted in a global dataset of 116,594 locations occurrence or prospect deposits, of which 74% were within the US. From these data we created a global map of the number of unexploited deposits within a 50 $km^2$ resolution. Due to sampling bias towards the US, we area-ranked from 1-100 the number of mining occurrences per cell within the US separately from non-US regions; the resulting US and non-US grids were then merged to produce one final mining development threat map.

**Global Map of Future Mining Development Threat:**

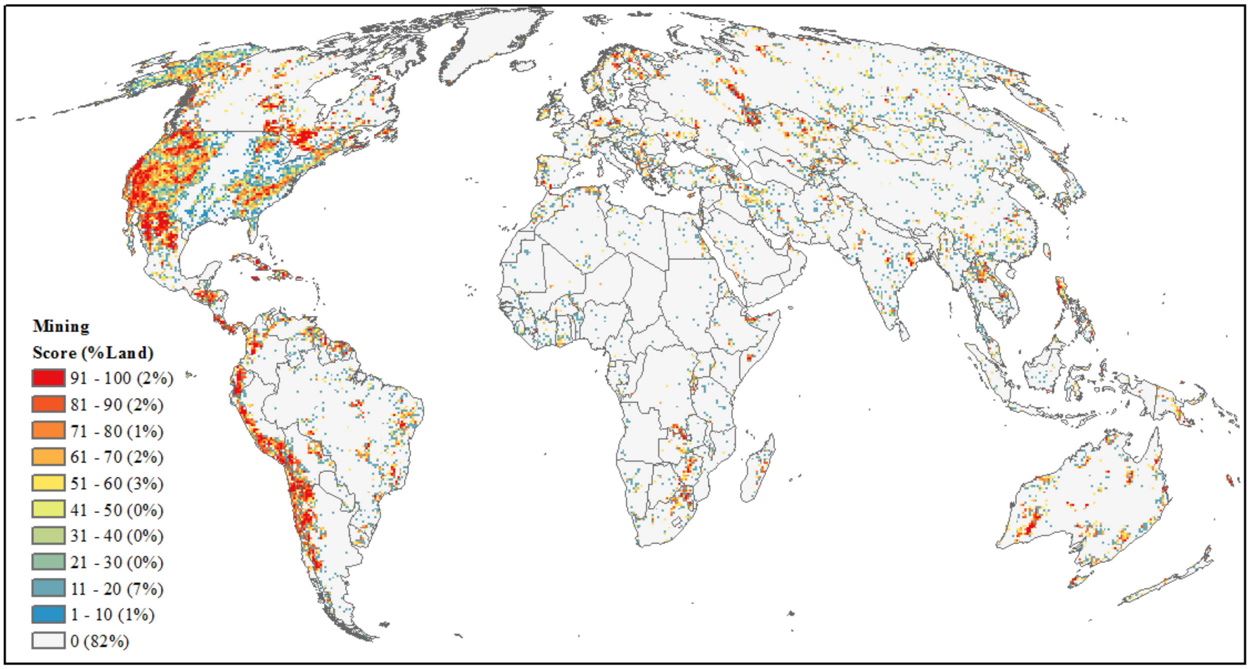


**Detailed Data Processing Steps:**

1. Created a global mineral occurrence point database based on three global sources.
    a. Downloaded USGS Mineral Resources Database (MRDS) (US Geological Survey, 2005) and created a global mineral occurrence dataset.
        i. Using the Development status field, selected only those points with the attribution of Occurrence or Prospect (Table 1), which represented deposits where little to no production has occurred (103,344 points were selected out of 305,011)
        ii. Removed those points with a commodity listing of only oil, gas, geothermal or water (removed 714 points)
        iii. Removed duplicate points with the same location and commodity type (removed 5746 points)
        iv. Final points used from USGS MRDS in global mineral occurrence database = 96,884.

**Table 1. Definitions for development status field within MRDS**

| Value | Description |
|---|---|
| Occurrence | Ore mineralization in outcrop, shallow pit or pits, or isolated drill hole. Grade, tonnage, and extent of mineralization essentially unknown. No production has taken place and there has been no or little activity since discovery with the possible exception of routine claim maintenance. |
| Prospect | A deposit that has gone beyond the occurrence stage. That is subsequent work such as surface trenching, adits, or shafts, drill holes, extensive geophysics, geochemistry, and/or geologic mapping has been carried out. Enough work has been done to at least estimate grade and tonnage. The deposits may or may not have undergone feasibility studies that would lead to a decision on going into production. |
| Producer | A mine in production at the time the data was entered. An intermittent producer |

| | |
|---|---|
| | that produces on demand or seasonally with variable lengths of inactivity is considered a producer. |
| Past Producer | A mine formerly operating that has closed, where the equipment or structures may have been removed or abandoned. |
| Plant | A processing plant (smelter, refiner, beneficiation, etc.) that may or may not be currently producing at the time of data entry. A plant will have no geological information associated with it. |
| Unknown | At the time of data entry, either the development status was unknown or the data source this record came from did not specify this value. |

b. Downloaded all data from the 2011 USGS Deposits Update (Causey et al., 2009; Cox et al., 2007; Singer et al., 2008) and added data to global mineral occurrence database.
   i. Removed all points related to current or past mining activity
   ii. Removed duplicate locations from MRDS
   iii. Points added to global mineral occurrence database created in step 1:
      1. Causey et al. (2009): 11,741 points
      2. Cox et al. (2007): 738 points
      3. Singer et al. (2008): 690 points.

c. Downloaded all nine datasets from the World Minerals Geoscience Database (Geologic Survey of Canada, 2005) (see Table 2 for names and data access links for points added to global mineral occurrence database).
   i. Combined all nine datasets
   ii. Removed any duplicates from previous sources (i.e. MRDS and 2011 Deposits Update)
   iii. Added 7310 points.

**Table 2. Name and data link of the nine datasets supporting World Minerals Geoscience Database**

| Name | Link |
|---|---|
| Mississippi Valley type Zn-Pb deposits | http://apps1.gdr.nrcan.gc.ca/gsc_minerals/zip/MVT.zip |
| Sedimentary exhalative Pb-Zn deposits | http://apps1.gdr.nrcan.gc.ca/gsc_minerals/zip/Sedex.zip |
| Lode Au deposits | http://apps1.gdr.nrcan.gc.ca/gsc_minerals/zip/AuWorld.zip |
| Volcanogenic massive sulfide deposits | http://apps1.gdr.nrcan.gc.ca/gsc_minerals/zip/vms.zip |
| Sediment-hosted Cu deposits | http://apps1.gdr.nrcan.gc.ca/gsc_minerals/zip/Sedcu.zip |
| Fe oxide+/-Cu+/-Au+/-U deposits | http://apps1.gdr.nrcan.gc.ca/gsc_minerals/zip/FeCuAu.zip |
| Porphyry Cu+/-Mo+/-Au deposits | http://apps1.gdr.nrcan.gc.ca/gsc_minerals/zip/Porph.zip |
| Ni+/-PGE+/-Cr deposits | http://apps1.gdr.nrcan.gc.ca/gsc_minerals/zip/NiPGECr.zip |
| Tin-Tungsten (Sn-W) deposits | http://apps1.gdr.nrcan.gc.ca/gsc_minerals/zip/SnW.zip |

2. Selected all points from the compiled global mineral occurrence database that were located on land. Land was identified using GADM Ver2, Level 0 country data (Hijmans Lab, 2012). This resulted in 116,594 points being selected.
3. Projected locations to a Mollweide projection.
4. Created raster summarizing the number of points within each 50 $km^2$. Grid cell values ranged from 1-828.
5. Separated raster into two distinct raster datasets: US and Non-US with grid cell values ranging from 1-824 and 1-207, respectively.
6. Area-ranked each raster from 1-100 based on the cell values (i.e. occurrence counts).
7. Merged two normalized raster datasets together to produce an overall global development threat from mining.

**Data Access:** http://s3.amazonaws.com/DevByDesign-Web/MappingAppsVer2/DevRisk/index.html

**Citation:** Oakleaf JR, Kennedy CM, Baruch-Mordo S, West PC, Gerber JS, Jarvis L, Kiesecker J (2015) A world at risk: Aggregating development trends to forecast global habitat conversion. PLoS ONE.

**Contact for Development Risk Data:**
Jim Oakleaf, Conservation Geographer
Development by Design, The Nature Conservancy
joakleaf@tnc.org

**References:**

British Geological Survey. (2012). *World Mineral Production: 2008-2012* (p. 118). Retrieved from https://www.bgs.ac.uk/downloads/start.cfm?id=2897

Causey, J. D., Galloway, J. P., & Zientek, M. L. (2009). An index to PGE-Ni-Cr deposits and occurrences in selected mineral-occurrence databases: U.S. Geological Survey Open-File Report 2009-1045. Retrieved June 15, 2013, from http://pubs.usgs.gov/of/2009/1045/

Cox, D. P., Lindsey, D. A., Singer, D. A., Moring, B. C., & Diggles, M. F. (2007). Sediment-Hosted Copper Deposits of the World: Deposit Models and Database: U.S. Geological Survey Open-File Report 03-107. Retrieved June 14, 2013, from http://pubs.usgs.gov/of/2003/of03-107/

Geologic Survey of Canada. (2005). World Geoscience Database Projects. Retrieved January 15, 2013, from at http://apps1.gdr.nrcan.gc.ca/gsc_minerals/index.phtml?language=en-CA

Hijmans Lab. (2012). GADM database of Global Administrative Areas - Ver 2. Retrieved January 15, 2013, from http://www.gadm.org

Kesler, S. E. (2007). Mineral Supply and Demand into the 21st Century. In *Workshop on Deposit Modeling, Mineral Resource Assessment, and their Role in Sustainable Development* (p. 8). Retrieved from http://pubs.usgs.gov/circ/2007/1294/reports/paper9.pdf

Schulz, K. J., & Briskey, J. A. (2003). USGS Fact Sheet 53-03: USGS Mineral Resources Program: The Global Mineral Resource Assessment Project. Retrieved April 15, 2014, from http://pubs.usgs.gov/fs/fs053-03/fs053-03.html

Singer, D. A., Berver, V. I., & Moring, B. . (2008). Porphyry copper deposits of the world–Database and grade and tonnage models: U.S. Geological Survey Open-File Report 2008-1155. Retrieved June 14, 2013, from http://pubs.usgs.gov/of/2008/1155/

US Geological Survey. (2005). Mineral Resources Data System (MRDS). Retrieved June 04, 2013, from http://mrdata.usgs.gov/mrds/

## *Future Development Threat for Utility-scaled Solar Power*

**Resource Description:** Utility-scaled solar power produces electricity from the sun's energy using two main types of technologies; concentrating solar power (CSP) and photovoltaic (PV). CSP relies on mirrors to heat liquids which are then run through a standard generator to produce electricity while PV technologies are panels which directly convert sunlight to electricity using semiconductor materials (US Department of Energy, 2008). Site selection for solar power development is dependent on solar radiation and is measured by Global Horizontal Irradiance (GHI). GHI is comprised of the total direct normal irradiance (DNI) and diffused horizontal irradiance (DHI) with GHI being mostly comprised of DNI on sunny days and DHI on cloudy days (3TIER, 2014b). Both GHI and DNI values are used in evaluating solar power development with other factors such as physical land characteristics and overall site feasibility. Due in part to volatile prices of non-renewable fuels and increasing awareness of carbon dioxide emissions related to power production using fossil fuels, world solar power generation has grown by more than ten-fold over the past 5 years (BP, 2013). Although solar power makes up less than 1% of global electricity demand, it is the fastest growing renewable electricity in the world (Center for Climate and Energy Solutions, 2012). There are over 50 countries currently producing solar power on a commercial basis with Germany being the lead producer (United Nations, 2012; US Energy Information Administration, 2012).

**Relative Future Threat Assessment - Methods Overview:** We used three main characteristics to estimate solar power development: 1) solar resources, 2) land suitability based on accessibility and physical restriction, and 3) economic feasibility based on electricity demand and infrastructure, following similar approaches as Bureau of Land Management - US Dept of Interior (2003); Lopez, Robers, Heimiller, Blair, & Porro (2012); US Department of Energy (2008). For solar resources, we used 3Tier's (2012) global, high resolution (3 km) irradiation data which measures GHI in watts per square meter ($W/m^2$). We created two resource grids, one with GHI values ≥ 182 $W/m^2$ for utility-scaled PV development and the other with GHI values ≥ 217 $W/m^2$ for CSP development (Lahmeyer International, 2010). When then normalized the PV and CSP values from 0 - 1 and summed these two resources together to produce an overall solar resource ranking. This ranking was then rescaled from 1 -100 with a 100 indicated the resources with the highest potential development for both PV and CSP.

We identified land suitability for solar power development by considering exclusion areas due to inaccessibility, human settlements, and topography. For accessibility we used GlobCover V2 land cover data (European Space Agency, 2008) and excluded rock and ice, artificial areas, water and wetlands from any potential development. We limited development to be only within 80 km of existing roads (Center for International Earth Science Information Network - CIESIN, 2013). Finally we excluded all mapped urban areas (Schneider, Friedl, & Potere, 2009) and slopes > 3 degrees (Lopez et al., 2012). All four criteria were combined creating an overall binary land suitability map.

Renewable energy development is economically feasible when in close proximity to demand and where existing infrastructure is available to support building sites and transporting energy (Bureau of Land Management - US Dept of Interior, 2003; US Department of Energy, 2008). Therefore, we created a feasibility mask by ranking straight-line distance to existing power sources and highly populated urban areas (i.e. demand centers). To identify power sources, we combined two datasets: one identifying all power-producing dams worldwide ($n$ = 1541) (Lehner et al., 2011) and another identifying carbon producing locations (CARMA) with associated power production values (Ummell, 2012). For the CARMA dataset we selected only those power plants able to produce at least five megawatts (MW) ($n$ = 15,782), which would be similar in size to an economically viable utility-scale power plant (Mendelsohn, Lowder, & Canavan, 2010). We created Euclidean distance surfaces from global power sources and large urban areas (Nordpil & United Nations - Population Division, 2010) and then normalized each distance from 0.001 to 1 based on inverse distance values. An overall distance rank was created by taking the average normalized distance score. Finally we doubled these overall distance scores for those countries already developing solar power (United Nations, 2012; US Energy Information Administration, 2012) to create final feasibility scores that were then normalized from 1 to 100 for the final feasibility ranking.

To create the final utility-scale solar power threat ranking, we multiplied the normalized solar resource values and feasibility rankings, limiting this calculation to only those areas designated as suitable. We then summed these scores at a 50 km resolution. Finally we area-ranked the summed values and normalized them from 1-100 to establish our final solar power development threat map.

**Global Map of Future Utility-scaled Solar Power Development Threat:**

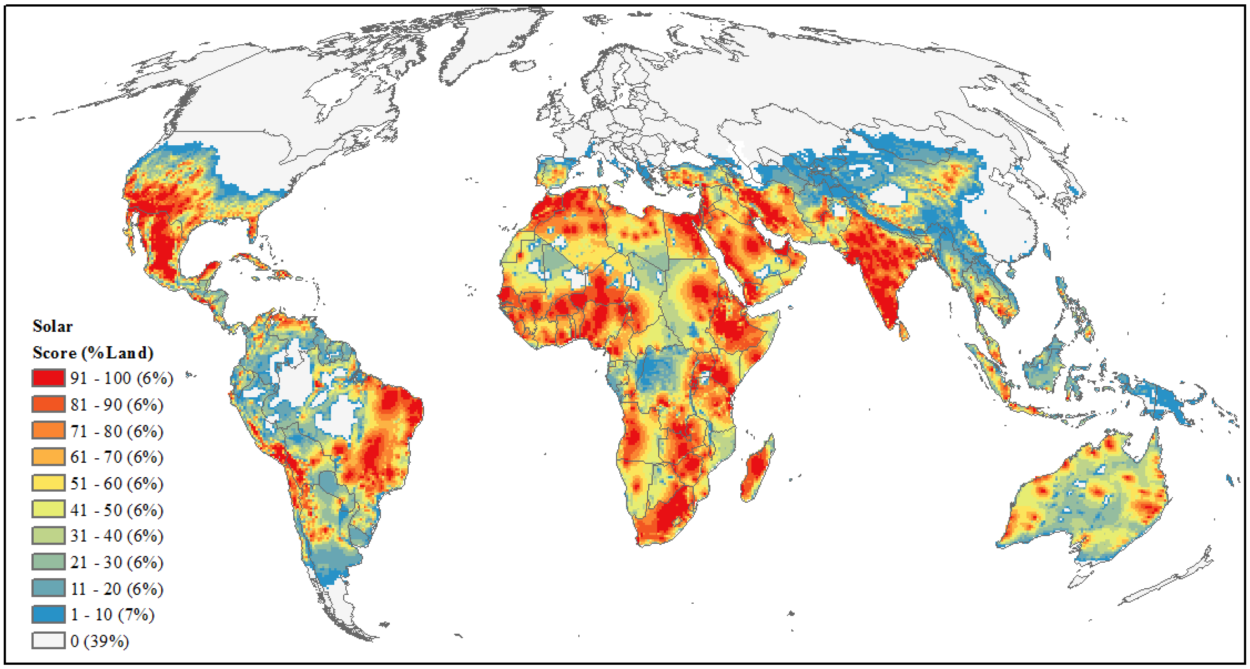


**Detailed Data Processing Steps:**

Task 1: Ranking for Potential Utility-scaled Solar Power Development

1. Obtained global horizontal irradiation (GHI) data at 3km resolution (3TIER, 2014a).
2. Projected raster data to Mollweide using bilinear interpretation.
3. Selected only cells with >217 W/m2 for CSP and >182 W/m2 for PV (Lahmeyer International, 2010).
4. Normalized CSP and PV values from 0.001-1.
5. Summed normalized values and re-normalized to 1-100 to produce one solar resource ranking.

Task 2: Land Suitability Mask for Solar Power Infrastructure

1. Slope mask: Selected land with slopes <= 3 degrees (Lopez et al., 2012).
    a. Slope in degrees was derived from GTOPO (USGS EROS Data Center, 1996), a global elevation raster dataset at a 1 km resolution
    b. All slopes <= 3 were set to 1 indicating suitable for solar power development.
2. Land cover mask: Selected only land cover appropriate for utility-scale solar energy development by removing artificial areas (i.e. urban areas, structures and pavement), water, wetlands, and rock and ice (Lopez et al., 2012).
    a. Selected appropriate land cover types using GlobCover V2 (European Space Agency, 2008) at 300m resolution, and based on urban extents at 500m resolution (Schneider et al., 2009)
    b. Set to 1 all land cover cells that were not urban areas and not classified as artificial areas, water, wetland and rock.
    c. Aggregated the suitable land cover derived in step 2b to a 900 m resolution raster summing suitable land cover cells

    d. Resampled 900m resolution raster to 1km using bilinear sampling
    e. Selected only those 1km cells with a value of 9 (i.e. fully developable) and set these cells to 1 indicating suitable land cover for solar power development.
3. Roads mask: Selected only areas within 50 miles or 80 km of existing roads (Bureau of Land Management - US Dept of Interior, 2003).
    a. Projected gROADS (Center for International Earth Science Information Network - CIESIN, 2013), a global roads dataset, to two-point equidistance
    b. Created a 1km resolution grid for all roads
    c. Calculated Euclidian distance from roads using 1km resolution up to 81 km
    d. Projected data to Mollweide using bilinear interpolation
    e. Selected cells less than or equal to 80km and set these cells to 1 indicating suitable for wind power development.
4. Created land suitability mask by selecting only cells that met all three criteria (i.e. slope mask = 1, land cover mask = 1, and roads mask = 1).

<u>Task 3: Feasibility Ranking</u>

1. Distance to demand centers rank.
    a. Projected the World Major Urban Areas (Nordpil & United Nations - Population Division, 2010) to two point equidistance projection
    b. Calculated an Euclidian distance surface at a 5 km resolution using the World Major Urban Areas
    c. Projected Euclidian distance surface to Mollweide projection using bilinear interpolation
    d. Calculated distance to demand centers rank by normalizing from 0-1 the cell values 1/Euclidian distance surface.
2. Distance to electric power generating sources rank.
    a. Global power plant location
        i. Using CARMA (Ummell, 2012), a global power plant locations database, selected those sites producing at least 5 megawatts of power, which is similar to an economically viable utility-scaled wind or solar power plant (n=15,782 sites selected out of 43,800)(Mendelsohn et al., 2010)
    b. Global hydro-power plants
        i. Using GRanD Database (Lehner et al., 2011), a global hydro dam database, selected all dams designated as producing hydroelectric power (n = 1541 dams out of a total of 6682 dams)
    c. Combined power plant locations and hydro-power dams into one global power producing locational database
    d. Projected all point locations from database to a two-point equidistance projection
    e. Calculated an Euclidian distance surface at a 5km resolution for all power producing locations
    f. Projected Euclidian distance surface to Mollweide projection using bilinear interpolation
    g. Calculated distance to current electric power generating sources rank by normalizing from 0-1 the cell values 1/Euclidian distance surface.

3. Created an overall distance score = (Distance to current electric power generating sources rank + Distance to demand centers rank) / 2.
4. Doubled overall distance scores for those cells located in countries already developing solar power (United Nations, 2012; US Energy Information Administration, 2012) to create final feasibility values.
5. Normalized final feasibility values from 1 – 100 to produce a final solar feasibility rank.

Task 4: Final Solar Power Threat Ranking

1. Multiplied the Solar Resource Ranking * Land Suitability Mask * Feasibility Ranking to produce a 1 km resolution raster.
2. Aggregated step 1 to 50 km resolution, summing values.
3. Area-ranked the aggregated values to 1-100 for final ranking.

**Data Access:** http://s3.amazonaws.com/DevByDesign-Web/MappingAppsVer2/DevRisk/index.html

**Citation:** Oakleaf JR, Kennedy CM, Baruch-Mordo S, West PC, Gerber JS, Jarvis L, Kiesecker J (2015) A world at risk: Aggregating development trends to forecast global habitat conversion. PLoS ONE.

**Contact for Development Risk Data:**

Jim Oakleaf, Conservation Geographer
Development by Design, The Nature Conservancy
joakleaf@tnc.org

**References:**

3TIER. (2014a). Global Solar Dataset 3km with units in W/m2. Retrieved February 15, 2014, from Personal contact

3TIER. (2014b). Glossary of Technical Renewable Energy Terminology. Retrieved April 10, 2014, from http://www.3tier.com/en/support/glossary/

BP. (2013). Statistical Review of World Energy 2013. Retrieved April 10, 2014, from http://www.bp.com/en/global/corporate/about-bp/energy-economics/statistical-review-of-world-energy-2013.html

Bureau of Land Management - US Dept of Interior. (2003). *Assessing the Potential for Renewable Energy on Public Lands* (p. 26). Retrieved from http://www.nrel.gov/docs/fy03osti/33530.pdf

Center for Climate and Energy Solutions. (2012). Solar Power. Retrieved April 10, 2014, from http://www.c2es.org/technology/factsheet/solar

Center for International Earth Science Information Network - CIESIN. (2013). Global Roads Open Access Data Set, Version 1 (gROADSv1). Retrieved January 05, 2013, from http://sedac.ciesin.columbia.edu/data/set/groads-global-roads-open-access-v1

European Space Agency. (2008). GlobCover Land Cover v2 2008 database. Retrieved February 15, 2012, from http://ionia1.esrin.esa.int/index.asp

Lahmeyer International. (2010). EmPower Utility Toolkit. Retrieved February 20, 2014, from http://www.empower-ph2.com/index.php?option=com_content&view=article&id=64&Itemid=41

Lehner, B., Liermann, C. R., Revenga, C., Vörösmarty, C., Fekete, B., Crouzet, P., … Wisser, D. (2011). High-resolution mapping of the world's reservoirs and dams for sustainable river-flow management. *Frontiers in Ecology and the Environment*, *9*(9), 494–502. doi:10.1890/100125

Lopez, A., Robers, B., Heimiller, D., Blair, N., & Porro, G. (2012). *U.S. Renewable Energy Technical Potentials: A GIS-Based Analysis* (p. 32). Retrieved from http://www.nrel.gov/docs/fy12osti/51946.pdf

Mendelsohn, M., Lowder, T., & Canavan, B. (2010). *Utility-Scale Concentrating Solar Power and Photovoltaic Projects: A Technology and Market Overview* (p. 55). Retrieved from http://www.nrel.gov/docs/fy12osti/51137.pdf

Nordpil, & United Nations - Population Division. (2010). World database of large urban areas, 1950-2050. Retrieved February 12, 2014, from http://nordpil.com/go/resources/world-database-of-large-cities/

Schneider, A., Friedl, M., & Potere, D. (2009). A new map of global urban extent from MODIS data. *Environmental Research Letters*, *4*. Retrieved from http://sage.wisc.edu/people/schneider/research/data.html

Ummell, K. (2012). CARMA revisited: an updated database of carbon dioxide emissions from power plants worldwide. Retrieved June 15, 2013, from http://carma.org/dig/

United Nations. (2012). Total Solar Electricity Production by Country. Retrieved December 15, 2013, from http://data.un.org/Data.aspx?q=solar&d=EDATA&f=cmID%3aES

US Department of Energy. (2008). *Assessing the Potential for Renewable Energy Development on DOE Legacy Management Lands* (p. 155). Retrieved from http://www.nrel.gov/docs/fy08osti/41673.pdf

US Energy Information Administration. (2012). Solar,Tide and Wave Electricty Generation by Country. Retrieved December 15, 2013, from http://www.eia.gov/cfapps/ipdbproject/iedindex3.cfm?tid=6&pid=36&aid=12&cid=regions&syid=2010&eyid=2010&unit=BKWH

USGS EROS Data Center. (1996). Global 30 Arc-Second Elevation Data Set. Retrieved October 15, 2013, from https://lta.cr.usgs.gov/GTOPO30

# *Future Development Threat for Unconventional Oil and Gas*

**Resource Description:** Unconventional oil and natural gas (OG) are resources distributed throughout a wide area but not concentrated within a reservoir (Behrens, Ratner, & Glover, 2011). Common unconventional resources include tight oil (e.g. oil sands and shale oil), shale gas, and coal-bed methane. These resources are extracted by advance drilling technologies and the practice of artificially fracturing formations (Ratner & Tiemann, 2014). The quantities of unconventional OG, similar to conventional OG, can be categorized as proven reserves or undiscovered resources with volumetric units in barrels for oil and liquid natural gas (NLG) and cubic feet for natural gas. Proven reserves are known OG volumes which are currently economically recoverable using current OG drilling (Behrens et al. 2011). Undiscovered resources are estimated OG volumes based on geological characteristics similar to currently producing geologic formations (Behrens et al., 2011), and their volumes are estimated by a computer simulation that predicts a range of possible volumes based on extraction probabilities (Charpentier & Cook, 2010). An overall mean estimated volume from these predictions is reported for each basin.

**Relative Future Threat Assessment - Methods Overview:** To produce a relative future development risk estimate for unconventional OG, we focused on resources found in shale and other sedimentary formations. We did not include any coal-bed methane (CBM) resource estimates because we estimated coal as a separate development threat. We relied on one global assessment (US Energy Information Administration, 2013) and a US specific assessment (US Geological Survey, 2012) to produce our relative future development threat estimate. For non-US regions, we georeferenced and digitized basin locations from the EIA Assessment (US Energy Information Administration, 2013) and linked resource volumes listed in the assessment to each basin. For the US assessment, we relied on digital spatial data from USGS (2012) and used estimates for continuous oil and gas, removing any basins assessed for CBM. Both datasets were combined to produce one complete global dataset. For each basin we calculated the billion barrels of oil equivalent (BBOE) for each resource (oil, gas, and natural gas liquids) and summed total resources together. Using the BBOE values of these basins, we then migrated these data to a raster dataset having a 50 $km^2$ cell size. For our analysis we only considered 50 $km^2$ cells overlapping at least 50% of the ranked basin and excluded any portion of the basin overlapping a marine environment. Finally we area-ranked from 1-100 cells having a BBOE value.

**Global Map of Future Unconventional Oil and Gas Development Threat:**

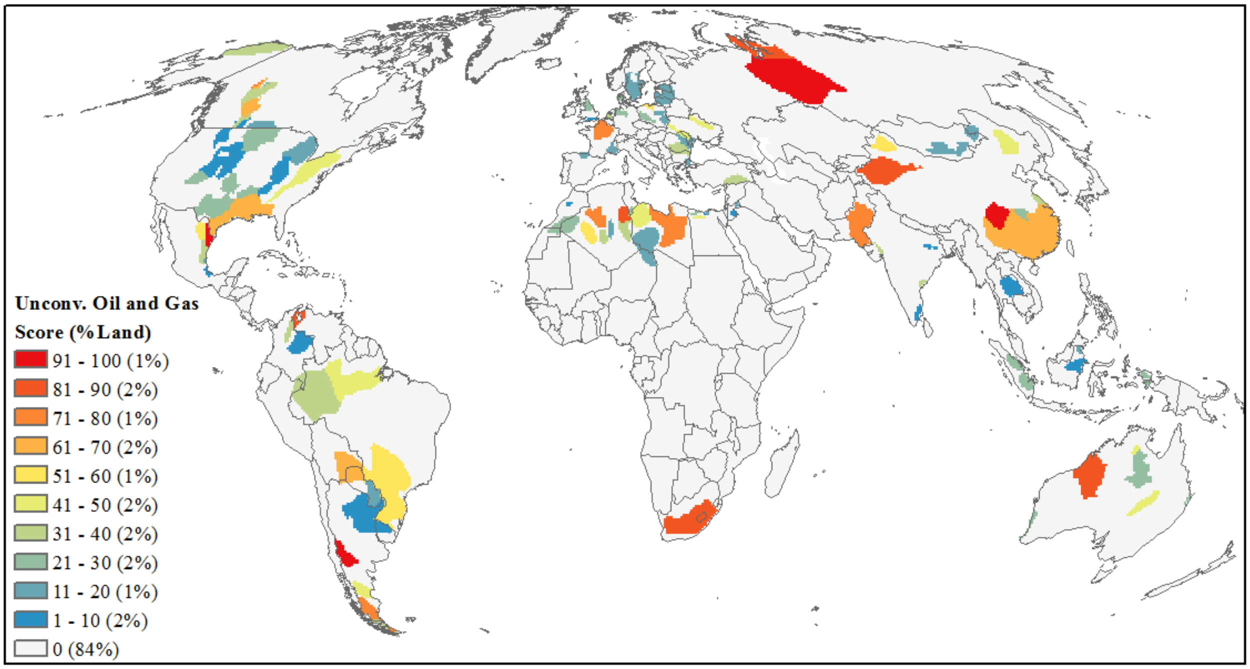


**Detailed Data Processing Steps:**

1. Global Data Development.
   a. Downloaded the EIA assessment (US Energy Information Administration, 2013)
   b. Geo-referenced and screen digitized basins from map images
   c. Labeled basin names
   d. Transferred from the report Attachment A: Size of Assessed Shale Gas and Shale Oil Resources, at Basin- and Formation-Levels to an excel table
   e. Used fields Technically Recoverable natural gas in trillion of cubic feet (tcf) and Technically Recoverable liquid natural gas in billions of barrels (bbl) to calculate an overall BBOE = tcf/6 + bbl for each basin.
2. US Data Development.
   a. Downloaded US province spatial data and volume estimates from USGS (US Geological Survey, 2012)
   b. From USGS excel worksheet, selected the *ContGas* table and using only shale gas volumes
   c. From USGS excel worksheet, selected the *ConOil* table
   d. Calculated BBOE values = # of billion barrels of oil + (# of trillion cubic feet of gas/6) + # of billion barrels of NLG.
3. Combined the global and US datasets.
4. Migrated the BBOE values associated with the polygon-based provinces to a raster format at a 50 $km^2$ cell resolution. Only cells with at least 50% of the province overlapping the cell were kept. Additionally our analysis removed any cell with 50% or more of the cell overlapping a marine environment.
5. Area-ranked from 1-100 cells having an BBOE value.

**Data Access:** [http://s3.amazonaws.com/DevByDesign-Web/MappingAppsVer2/DevRisk/index.html](http://s3.amazonaws.com/DevByDesign-Web/MappingAppsVer2/DevRisk/index.html)

**Citation:** Oakleaf JR, Kennedy CM, Baruch-Mordo S, West PC, Gerber JS, Jarvis L, Kiesecker J (2015) A world at risk: Aggregating development trends to forecast global habitat conversion. PLoS ONE.

**Contact for Development Risk Data:**

Jim Oakleaf, Conservation Geographer
Development by Design, The Nature Conservancy
joakleaf@tnc.org

**References:**

Behrens, C. E., Ratner, M., & Glover, C. (2011). *U . S . Fossil Fuel Resources : Terminology , Reporting , and Summary* (pp. 1–25). Retrieved from https://www.fas.org/sgp/crs/misc/R40872.pdf

Charpentier, R., & Cook, T. (2010). Improved USGS methodology for assessing continuous petroleum resources. *US Geological Survey Data Series*. Retrieved from http://pubs.usgs.gov/ds/547/downloads/DS547v2.pdf

Ratner, M., & Tiemann, M. (2014). *An overview of unconventional oil and natural gas: resources and federal actions*. Retrieved from http://www.fas.org/sgp/crs/misc/R43148.pdf

US Energy Information Administration. (2013). Technically Recoverable Shale Oil and Shale Gas Resources: An Assessment of 137 Shale Formations in 41 Countries Outside the United States . Retrieved October 15, 2013, from http://www.eia.gov/analysis/studies/worldshalegas/pdf/fullreport.pdf

US Geological Survey. (2012). National Oil and Gas Assessment 2012 Assessment Updates. Retrieved September 01, 2013, from http://energy.usgs.gov/OilGas/AssessmentsData/NationalOilGasAssessment/AssessmentUpdates.aspx

# *Future Development Threat for Urban Expansion*

**Resource Description:** Urban expansion is a major global driver of land use change with developing countries predicted to experience a triple in land area due to rural poor migrating to major cities and industrial countries seeing a continuing increase in low-density sprawl (Lincoln Institue of Land Policy, 2011). Urban land growth is expected to triple by 2030 relative to about 2000 with an estimated total of 1.8 million $km^2$ to be classified as urban globally (Angel, Parent, Civco, & Blei, 2011). Nearly half of the global increase in urban expansion is expected to occur in Asia (Seto, Güneralp, & Hutyra, 2012). While the overall amount of land expected to be converted to urban is less than 1%, urban expansion is likely to have significant impacts on biodiversity hotspots and carbon pools (Seto et al., 2012) and is predicted to contribute greatly to the loss of prime agricultural lands (Lincoln Institue of Land Policy, 2011).

**Relative Future Threat Assessment - Methods Overview:** To capture urban expansion, we used Seto et al. (2012) Global Urban Expansion probability layer, which maps probabilities of urban expansion globally to 2030 at a 5 km resolution based on global land cover circa 2000, projections of urban population, and gross domestic product (GDP) growth. Seto et al (2012) spatially distributed the amount of urban expansion via a spatially explicit land change model, which used slope, distance to roads, population density, and land cover as primary drivers of land change (see Seto et al 2012 for further details). To focus on future development threat, we excluded currently identified urban areas. To ensure consistency with our other threat layers, we calculated the mean probablity of urban expansion at a 50km resolution. We then area-ranked the mean probabilities from 1-100 after excluding zero values.

**Global Map of Future Urban Expansion Development Threat:**

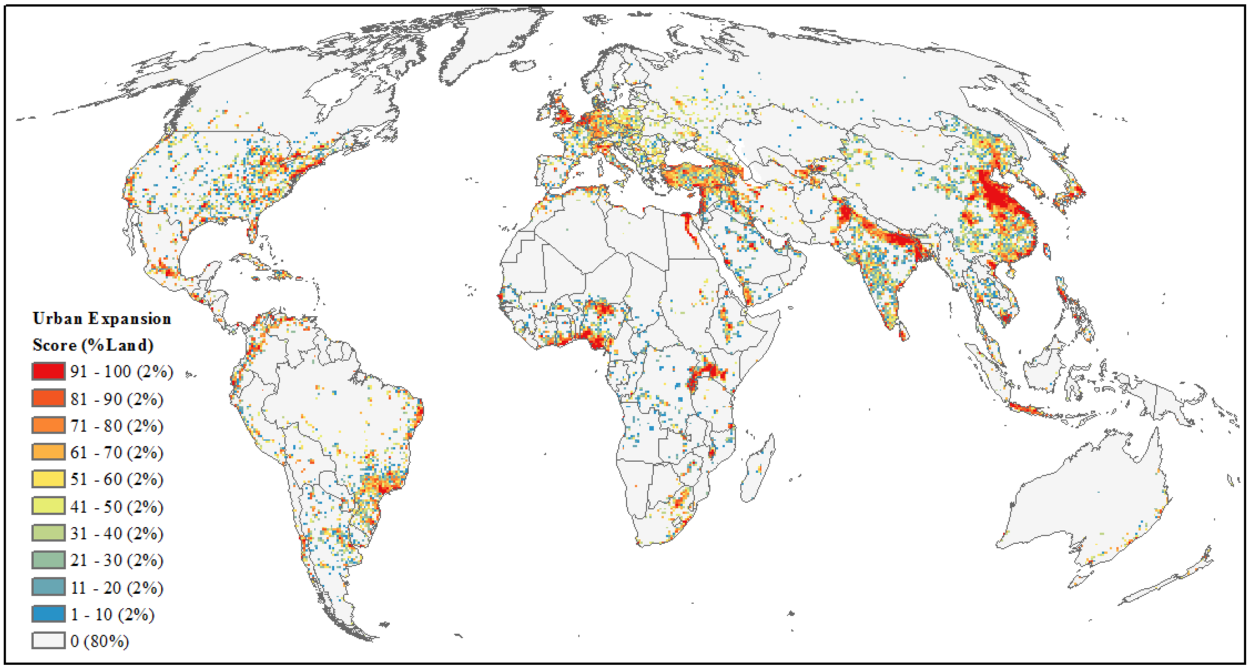


**Detailed Data Processing Steps:**

1. Downloaded from http://urban.yale.edu/DataResources.html , 2030 global urban expansion probability data at 5 km resolution (Seto et al., 2012).
2. Projected data to a Mollweide projection using a bilinear interpolation.
3. Set to null currently identified urban areas (value = 101), which left values ranging from 0 (no probable urban expansion in 2030) to 100.
4. Calculated mean of probabilities at a 50 km resolution.
5. Removed values with a mean probability of 0.
6. Area-ranked the aggregate means (excluding zeros) from 1-100.

**Data Access:** http://s3.amazonaws.com/DevByDesign-Web/MappingAppsVer2/DevRisk/index.html

**Citation:** Oakleaf JR, Kennedy CM, Baruch-Mordo S, West PC, Gerber JS, Jarvis L, Kiesecker J (2015) A world at risk: Aggregating development trends to forecast global habitat conversion. PLoS ONE.

**Contact for Development Risk Data:**

Jim Oakleaf, Conservation Geographer
Development by Design, The Nature Conservancy
joakleaf@tnc.org

**References:**

Angel, S., Parent, J., Civco, D. L., & Blei, A. M. (2011). *Makng Room for a Planet of Cities*. Retrieved from https://www.lincolninst.edu/pubs/dl/1880_1195_Angel PFR final.pdf

Lincoln Institue of Land Policy. (2011). Atlas of Urban Expansion. Retrieved April 10, 2014, from http://www.lincolninst.edu/subcenters/atlas-urban-expansion/

Seto, K. C., Güneralp, B., & Hutyra, L. R. (2012). Global forecasts of urban expansion to 2030 and direct impacts on biodiversity and carbon pools. *Proceedings of the National Academy of Sciences of the United States of America*, *109*(40), 16083–8. doi:10.1073/pnas.1211658109

## *Future Development Threat for Utility-scaled Wind Power*

**Resource Description:** Utility-scaled wind power uses a collection of wind turbines (i.e. wind farm) to generate electricity ranging anywhere from five megawatts (MW) to several hundred MW, which is then sold to utility companies (American Wind Energy Association, 2008). With the volatile prices of non-renewable fuels and increasing awareness of carbon dioxide emissions related to power production using fossil fuels, world wind power generation has more than doubled in the last four years and currently contributes 4% to the global electricity demand (World Wind Energy Association, 2014). There are over 103 countries currently producing wind power on a commercial basis with high growth rates being seen in Latin America, Eastern Europe and even Africa (World Wind Energy Association, 2014). Currently the two top producers of wind energy are China and US (US Energy Information Administration, 2012).

**Relative Future Threat Assessment - Methods Overview:** We used three main characteristics to estimate wind power development: 1) wind resources, 2) land suitability based on accessibility and physical restriction, and 3) economic feasibility based on electricity demand and infrastructure, following similar approaches as Bureau of Land Management - US Dept of Interior (2003); Lopez, Robers, Heimiller, Blair, & Porro (2012); US Department of Energy (2008). For wind resources, we used 3Tier's (2012) global, high resolution (i.e. 5 km) wind speed data which measures winds speeds in meters/second (m/s) at 80m above earth's surface. We limited our analyses to yearly average wind speeds ≥ 6.4 m/s, which are deemed most feasible for utility-scaled wind development (Bureau of Land Management - US Dept of Interior, 2003; US Department of Energy, 2008) which we then normalized values from 0.001 -1 with a 1 indicated the highest resource potential globally.

We identified land suitability for wind power development by considering exclusion areas due to inaccessibility, human settlements, and topography. For accessibility we used GlobCover V2 land cover data (European Space Agency, 2008) and excluded rock and ice, artificial areas, water and wetlands from any potential development. We limited development to be only within 80 km of an existing roads (Center for International Earth Science Information Network - CIESIN, 2013). Finally we excluded all mapped urban areas (Schneider, Friedl, & Potere, 2009) and slopes > 20 degrees(Lopez et al., 2012). All four criteria were combined creating an overall binary land suitability map.

Renewable energy development is economically feasible when in close proximity to demand and where existing infrastructure is available to support building sites and transporting energy (American Wind Energy Association, 2008; Bureau of Land Management - US Dept of Interior, 2003; US Department of Energy, 2008). Therefore, we created a feasibility mask by ranking straight-line distance to existing power sources and highly populated urban areas (i.e. demand centers). To identify power sources, we combined two datasets: one identifying all power-producing dams worldwide (*n* = 1541)(Lehner et al., 2011) and another identifying carbon producing locations (CARMA) with associated power production values (Ummell, 2012). For the CARMA dataset we selected only those power plants able to produce at least five megawatts (MW) (*n* = 15,782), which would be similar in size to an economically viable utility-scale power plant (Mendelsohn, Lowder, & Canavan, 2010). We created Euclidean distance surfaces from global power sources and large urban areas (Nordpil & United Nations - Population Division, 2010) and then normalized each distance from 0.001 to 1 based on the inverse distance value. An overall distance rank was created by taking the average normalized distance score. Finally we doubled these overall distance scores for those countries already developing wind power (United Nations, 2012; US Energy Information Administration, 2012) to create final feasibility scores that were then normalized values from 0.001 to 1 for the final feasibility ranking.

To create the final utility-scale wind power threat ranking, we multiplied the normalized wind resource values and feasibility ranks, limiting this calculation to only those areas designated as suitable and that met the required wind speed cutoff. We then summed these scores at a 50 km resolution. Finally we area-ranked the summed values and normalized them from 1-100 to establish our final wind power development threat map.

**Global Map of Future Utility-scaled Wind Power Development Threat:**

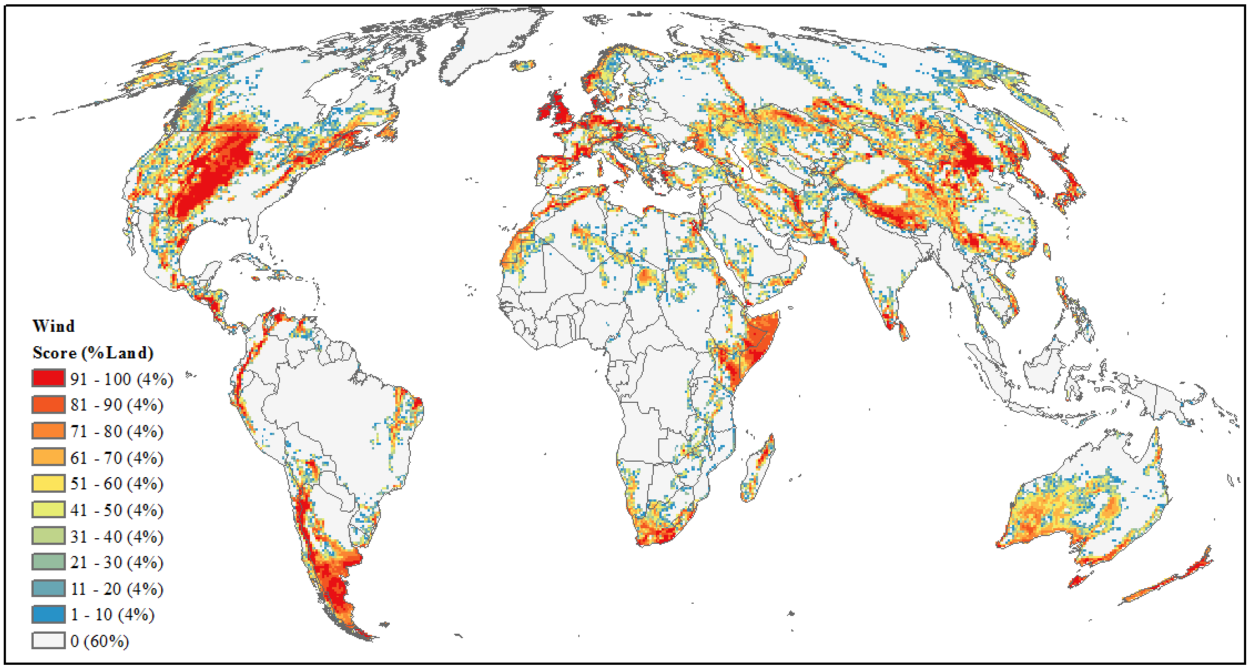


**Detailed Data Processing Steps:**

Task 1: Ranking for Potential Utility-Scaled Development

1. Obtained global wind speed data at 5km resolution (3TIER, 2014).
2. Projected raster data to Mollweide using bilinear interpretation.
3. Selected only cells with wind speeds ≥6.4 m/s, which are necessary to support utility-scale wind development (Bureau of Land Management - US Dept of Interior, 2003; US Department of Energy, 2008).
4. Wind speed values were min/max normalized and scaled from 0.001 – 1 to produce one wind resource ranking.

Task 2: Land Suitability Mask for Wind Power Infrastructure

1. Slope mask: Selected land with slopes <= 20 degrees (Lopez et al., 2012)
   a. Slope in degrees was derived from GTOPO (USGS EROS Data Center, 1996), a global elevation raster dataset at a 1 km resolution
   b. All slopes <= 20 were set to 1 indicating suitable for wind power development.
2. Land cover mask: Selected only land cover appropriate for utility-scale wind energy development by removing artificial areas (i.e. urban areas, structures and pavement), water, wetlands, and rock and ice (Lopez et al., 2012).
   a. Selected appropriate land cover types using GlobCover V2 (European Space Agency, 2008) and urban extents (Schneider et al., 2009)
   b. Set to 1 all land cover cells that were not in urban areas not and classified as artificial areas, water, wetland and rock
   c. Aggregated the suitable land cover derived in step 2b from 300 m to a 900 m resolution raster summing suitable land cover cells
   d. Resampled 900m resolution raster to 1km using bilinear sampling

    e. Selected only those 1km cells with a value of 9 (i.e. fully developable) and set these cells to 1 indicating suitable land cover for wind power development.
3. Roads mask: Selected only areas within 50 miles or 80 km of existing roads (Bureau of Land Management - US Dept of Interior, 2003).
    a. Projected gROADS (Center for International Earth Science Information Network - CIESIN, 2013), a global roads dataset, to two-point equidistance
    b. Created a 1km resolution grid for all roads
    c. Calculated Euclidian distance from roads using 1km resolution up to 81 km
    d. Projected data to Mollweide using bilinear interpolation
    e. Selected cells less than or equal to 80km and set these cells to 1 indicating suitable for wind power development.
4. Created land suitability mask by selecting only cells that met all three criteria (i.e. slope mask = 1, land cover mask = 1, and roads mask = 1).

<u>Task 3: Feasibility Ranking</u>

1. Distance to demand centers rank.
    a. Projected the World Major Urban Areas (Nordpil & United Nations - Population Division, 2010) to two point equidistance projection
    b. Calculated an Euclidian distance surface at a 5 km resolution using the World Major Urban Areas
    c. Projected Euclidian distance surface to Mollweide projection using bilinear interpolation
    d. Calculated distance to demand centers rank by normalizing from 0-1 the cell values 1/Euclidian distance surface.
2. Distance to electric power generating sources rank.
    a. Global power plant location
        i. Using CARMA (Ummell, 2012), a global power plant locations database, selected those sites producing at least 5 megawatts of power which is similar to an economically viable utility-scaled wind or solar power plant (n=15,782 sites selected out of 43,800)(Mendelsohn et al., 2010)
    b. Global hydro-power plants
        i. Using GRanD Database (Lehner et al., 2011), a global hydro dam database, selected all dams designated by database as producing hydroelectric power (n = 1541 dams out of a total of 6682 dams)
    c. Combined power plant locations and hydro-power dams into one global power producing locational database
    d. Projected all point locations from database to a two-point equidistance projection
    e. Calculated an Euclidian distance surface at a 5km resolution for all power producing locations
    f. Projected Euclidian distance surface to Mollweide projection using bilinear interpolation
    g. Calculated distance to current electric power generating sources rank by normalizing from 0-1 the cell values 1/Euclidian distance surface.

3. Created an overall distance score = (Distance to current electric power generating sources rank + Distance to demand centers rank) / 2.
4. Doubled overall distance scores for those cells located in countries already developing wind power (United Nations, 2012; US Energy Information Administration, 2012) to create final feasibility values.
5. Normalized final feasibility values from 0 – 1 to produce a final wind feasibility rank.

Task 4: Final Wind Power Threat Ranking

1. Multiplied the Wind Speed Ranking * Land Suitability Mask * Feasibility Ranking to produce a 1 km resolution raster.
2. Aggregated step 1 to 50 km resolution, summing values.
3. Area-ranked the aggregated values to 1-100 for final ranking.

**Data Access:** http://s3.amazonaws.com/DevByDesign-Web/MappingAppsVer2/DevRisk/index.html

**Citation:** Oakleaf JR, Kennedy CM, Baruch-Mordo S, West PC, Gerber JS, Jarvis L, Kiesecker J (2015) A world at risk: Aggregating development trends to forecast global habitat conversion. PLoS ONE.

**Contact for Development Risk Data:**

Jim Oakleaf, Conservation Geographer
Development by Design, The Nature Conservancy
joakleaf@tnc.org

**References:**

3TIER. (2014). Onshore Global Wind Speeds at 80m Height. Retrieved February 15, 2014, from personal contact

American Wind Energy Association. (2008). *Wind Energy Siting Handbook* (p. 178). Retrieved from http://www.awea.org/Issues/Content.aspx?ItemNumber=5726

Bureau of Land Management - US Dept of Interior. (2003). *Assessing the Potential for Renewable Energy on Public Lands* (p. 26). Retrieved from http://www.nrel.gov/docs/fy03osti/33530.pdf

Center for International Earth Science Information Network - CIESIN. (2013). Global Roads Open Access Data Set, Version 1 (gROADSv1). Retrieved January 05, 2013, from http://sedac.ciesin.columbia.edu/data/set/groads-global-roads-open-access-v1

European Space Agency. (2008). GlobCover Land Cover v2 2008 database. Retrieved February 15, 2012, from http://ionia1.esrin.esa.int/index.asp

Lehner, B., Liermann, C. R., Revenga, C., Vörösmarty, C., Fekete, B., Crouzet, P., … Wisser, D. (2011). High-resolution mapping of the world's reservoirs and dams for sustainable river-flow management. *Frontiers in Ecology and the Environment*, *9*(9), 494–502. doi:10.1890/100125

Lopez, A., Robers, B., Heimiller, D., Blair, N., & Porro, G. (2012). *U.S. Renewable Energy Technical Potentials: A GIS-Based Analysis* (p. 32). Retrieved from http://www.nrel.gov/docs/fy12osti/51946.pdf

Mendelsohn, M., Lowder, T., & Canavan, B. (2010). *Utility-Scale Concentrating Solar Power and Photovoltaic Projects: A Technology and Market Overview* (p. 55). Retrieved from http://www.nrel.gov/docs/fy12osti/51137.pdf

Nordpil, & United Nations - Population Division. (2010). World database of large urban areas, 1950-2050. Retrieved February 12, 2014, from http://nordpil.com/go/resources/world-database-of-large-cities/

Schneider, A., Friedl, M., & Potere, D. (2009). A new map of global urban extent from MODIS data. *Environmental Research Letters*, *4*. Retrieved from http://sage.wisc.edu/people/schneider/research/data.html

Ummell, K. (2012). CARMA revisited: an updated database of carbon dioxide emissions from power plants worldwide. Retrieved June 15, 2013, from http://carma.org/dig/

United Nations. (2012). Toal Wind Electricity Production by Country. Retrieved December 15, 2013, from http://data.un.org/Data.aspx?q=wind&d=EDATA&f=cmID:EW

US Department of Energy. (2008). *Assessing the Potential for Renewable Energy Development on DOE Legacy Management Lands* (p. 155). Retrieved from http://www.nrel.gov/docs/fy08osti/41673.pdf

US Energy Information Administration. (2012). Wind Electricty Generation by Country. Retrieved December 15, 2013, from http://www.eia.gov/cfapps/ipdbproject/iedindex3.cfm?tid=6&pid=37&aid=12&cid=regions&syid=2012&eyid=2012&unit=BKWH

USGS EROS Data Center. (1996). Global 30 Arc-Second Elevation Data Set. Retrieved October 15, 2013, from https://lta.cr.usgs.gov/GTOPO30

World Wind Energy Association. (2014). World Wind Energy - Statistics. Retrieved April 09, 2014, from http://www.wwindea.org/home/index.php?option=com_content&task=blogcategory&id=21&Itemid=43